Science Advances
AAAS

Supplementary Materials for

Alu complementary DNA is enriched in atrophic macular degeneration and triggers retinal pigmented epithelium toxicity via cytosolic innate immunity

Shinichi Fukuda, Siddharth Narendran, Akhil Varshney, Yosuke Nagasaka, Shao-bin Wang, Kameshwari Ambati, Ivana Apicella, Felipe Pereira, Benjamin J. Fowler, Tetsuhiro Yasuma, Shuichiro Hirahara, Reo Yasuma, Peirong Huang, Praveen Yerramothu, Ryan D. Makin, Mo Wang, Kirstie L. Baker, Kenneth M. Marion, Xiwen Huang, Elmira Baghdasaryan, Meenakshi Ambati, Vidya L. Ambati, Daipayan Banerjee, Vera L. Bonilha, Genrich V. Tolstonog, Ulrike Held, Yuichiro Ogura, Hiroko Terasaki, Tetsuro Oshika, Deepak Bhattarai, Kyung Bo Kim, Sanford H. Feldman, J. Ignacio Aguirre, David R. Hinton, Nagaraj Kerur, Srinivas R. Sadda, Gerald G. Schumann, Bradley D. Gelfand, Jayakrishna Ambati*

*Corresponding author. Email: ja9qr@virginia.edu

Published 29 September 2021, *Sci. Adv.* **7**, eabj3658 (2021)
DOI: 10.1126/sciadv.abj3658

This PDF file includes:

Figs. S1 to S11

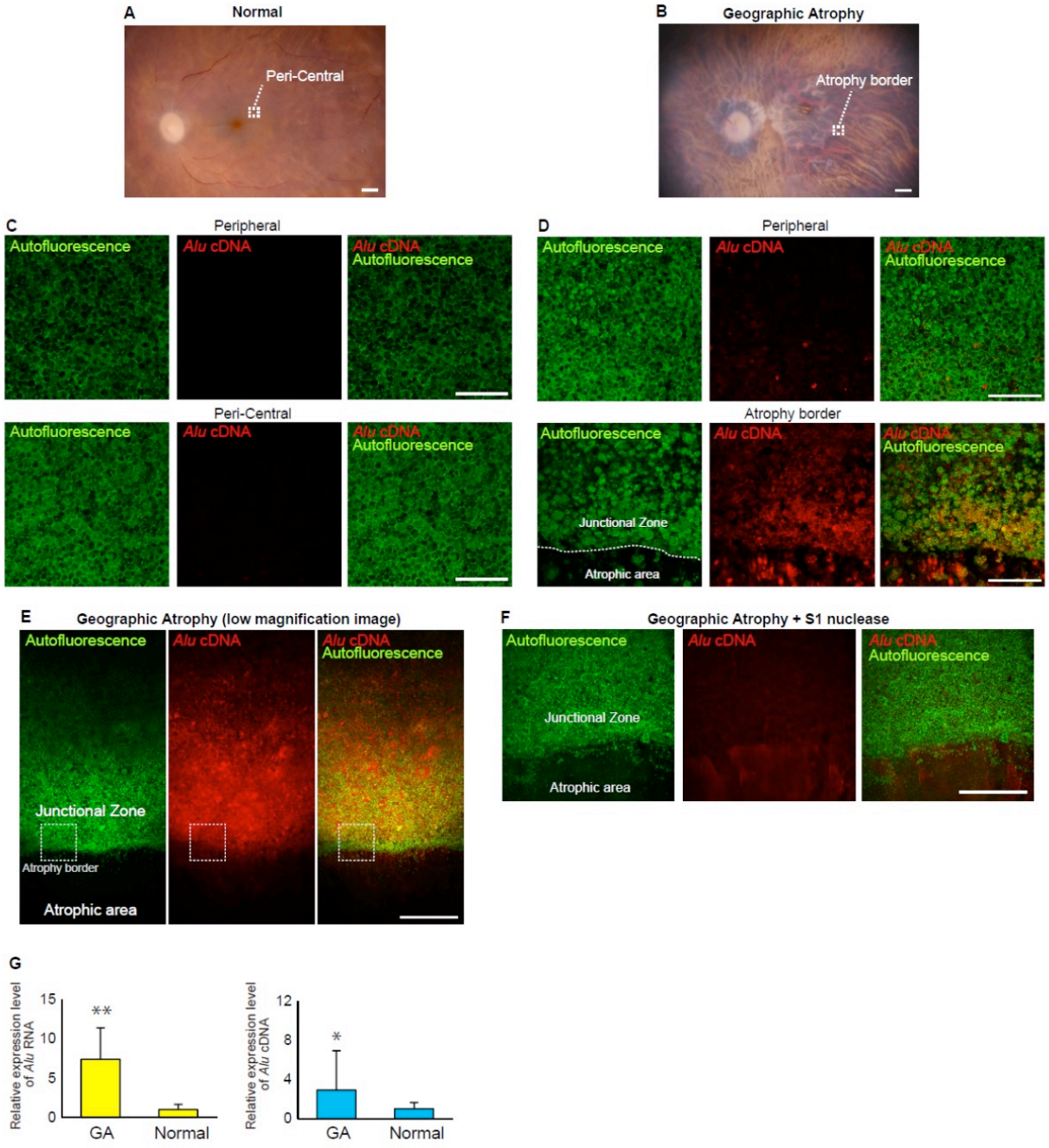

Fig. S1. *Alu* cDNA accumulation in human GA RPE. (A and **B)** Ex vivo fundus photographs of retina from a normal human donor eye **(A)** and an eye with geographic atrophy (GA) **(B)**. Scale bars, 1 mm. **(C, D)** In situ hybridization of RPE whole mounts with *Alu* cDNA-specific probes in peripheral and peri-central areas of normal eyes **(C)**, and in the junctional zone and peripheral areas of GA eyes **(D)**. Insets show higher magnification. Red, *Alu* cDNA; green, autofluorescence. A few scattered foci of *Alu* cDNA were present in the peripheral disease-free area in GA **(D)**. Red, *Alu* cDNA; green, autofluorescence of RPE cells. Scale bars, 100 μm. The

junctional zone is a 500 μm annulus circumscribing the atrophic region. Atrophy border is the interface of the atrophic region and the junctional zone. **(E)** Low magnification of whole mount in situ hybridization of *Alu* cDNA (red) in the RPE of a GA eye showed enrichment in the atrophic border and junctional zone. Scale bars, 500 μm. **(F)** Whole mount in situ hybridization of *Alu* cDNA (red) in the RPE of a GA eye showed loss of the red signal following treatment with single-stranded specific S1 nuclease. Scale bars, 500 μm. **(G)** Densitometry of the bands in Fig. 1E corresponding to northern blotting of *Alu* RNA and equator blotting of *Alu* cDNA in the macula normalized to loading control (U6) with the mean densitometry ratio of macular RPE of normal eyes set to 1.0. ** $P < 0.01$, * $P < 0.05$ by Mann-Whitney U test.

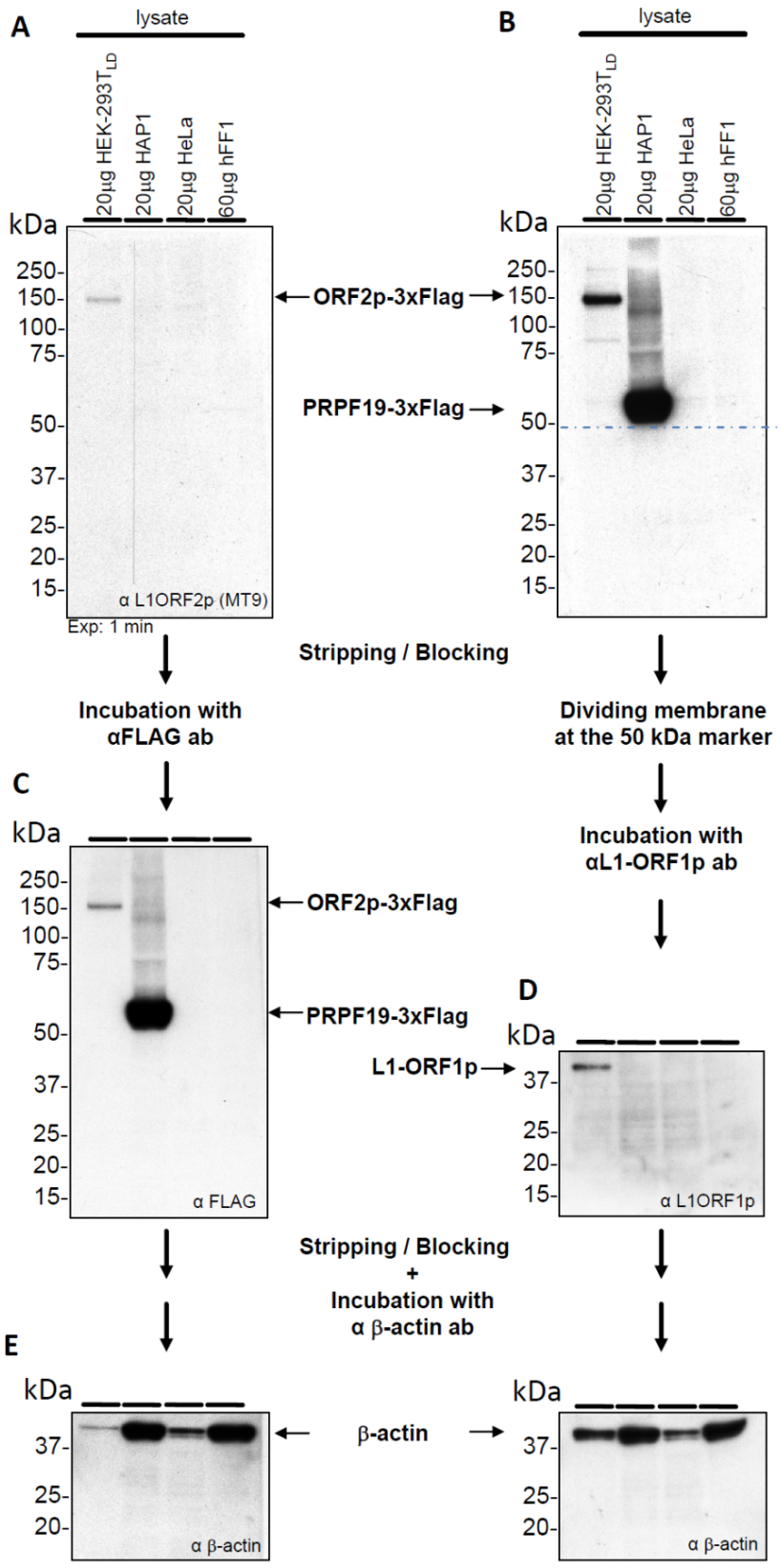
A
lysate
20µg HEK-293T$_{LD}$
20µg HAP1
20µg HeLa
60µg hFF1
kDa
250-
150-
100-
75-
50-
37-
25-
20-
15-
α L1ORF2p (MT9)
Exp: 1 min
ORF2p-3xFlag
PRPF19-3xFlag
B
lysate
20µg HEK-293T$_{LD}$
20µg HAP1
20µg HeLa
60µg hFF1
kDa
250-
150-
100-
75-
50-
37-
25-
20-
15-
Stripping / Blocking
Incubation with
αFLAG ab
Dividing membrane
at the 50 kDa marker
C
kDa
250-
150-
100-
75-
50-
37-
25-
20-
15-
α FLAG
ORF2p-3xFlag
PRPF19-3xFlag
Incubation with
αL1-ORF1p ab
D
kDa
L1-ORF1p
37-
25-
20-
15-
α L1ORF1p
Stripping / Blocking
+
Incubation with
α β-actin ab
E
kDa
37-
25-
20-
α β-actin
β-actin
kDa
37-
25-
20-
α β-actin

Fig. S2. Immunoblot detection of human L1-ORF2p-3xFlag ectopically expressed from the pMT302 plasmid in HEK-293T$_{LD}$ cells (53) supports specificity of the αL1-ORF2p MT9 antibody (47). The ~150 kDa L1-ORF2p-3xFlag protein expressed in HEK-293T$_{LD}$ cells (gift of John LaCava, University of Groningen, The Netherlands) is specifically detected with both the MT9 antibody (**A**) and the αFLAG-tag antibody **(B, C**). Cell extracts from transgenic HAP1 cells (gift of Csaba Miskey. Paul-Ehrlich-Institute) constitutively expressing the 3xFlag-tagged PRPF19 protein (~ 55 kDa) were loaded as positive control for FLAG-tag expression and detection. Testing for the presence of the 40-kDa L1-ORF1p (**D**) served as positive control for ectopic expression of pMT302 in HEK-293T$_{LD}$ cells. β-actin expression (42 kDa; E) served as loading control. Cell lysates from human HeLa cells and foreskin fibroblasts (hFF1) did not include any detectable amounts of L1 proteins.

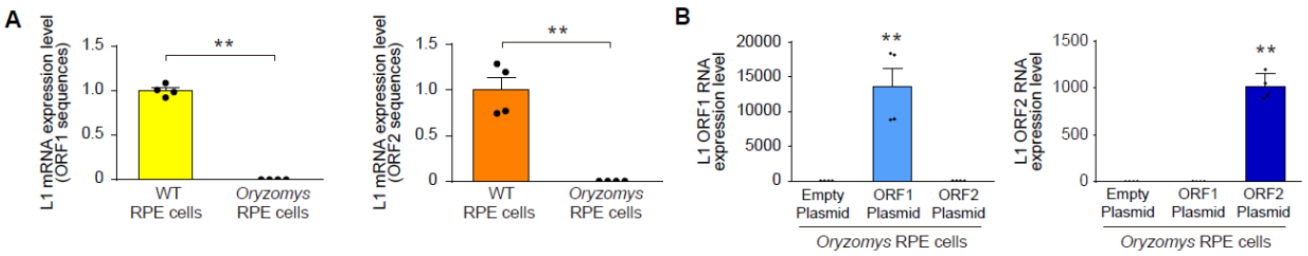

Fig. S3. Absence of detectable rat L1 mRNA in *Oryzomys palustris*. (A) Quantification of endogenous mRNAs harboring L1 ORF1 and L1 ORF2 sequences in RPE cells from WT rats (*R. norvegicus*) and from *O. palustris* by real-time PCR. L1 mRNAs are detected in WT rat RPE cells but not in *O. palustris* RPE cells. ** $P < 0.01$ by Mann-Whitney U test. Error bars show SEM. $n = 4$. **(B)** Real-time PCR analysis of L1 ORF1 and ORF2 RNA abundance in *O. palustris* RPE cells transfected with plasmids encoding either rat L1 ORF1 or rat ORF2. ** $P < 0.01$ by Mann-Whitney U test. Error bars show SEM. $n = 4$.

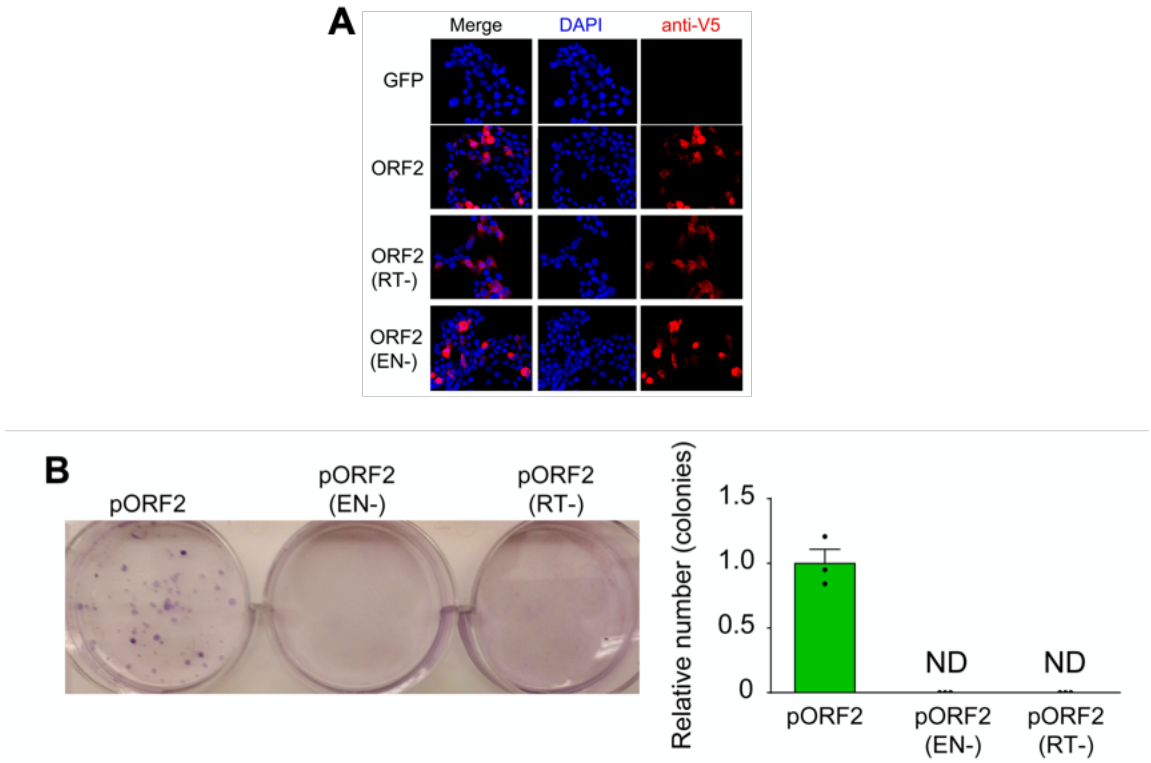

Fig. S4. L1 ORF2p-encoded endonuclease and reverse transcriptase activities are required for *Alu* retrotransposition in a trans-mobilization assay in HeLa-HA cells. (A) Fluorescence imaging of HeLa-HA cells transfected with plasmids encoding GFP, V5-tagged rat L1 ORF2, V5-tagged rat L1 ORF2 (EN–), or V5-tagged L1 ORF2 (RT–) mutant proteins and stained with DAPI and anti-V5 antibody. (**B**) *Alu* retrotransposition assays of plasmid-encoded rat L1 ORF2p, or endonuclease-deficient (EN–) or transcriptase-deficient (RT–) mutants. $n = 3$. *$P < 0.05$ by Mann-Whitney U test. Error bars show SEM. ND, not detected.

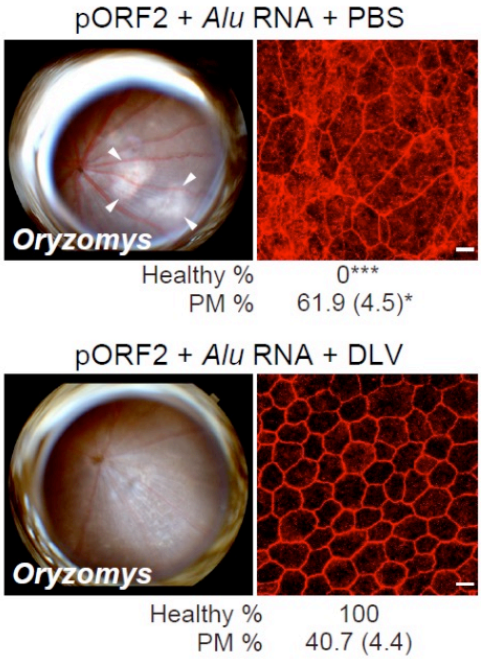

Fig. S5. Rat L1 ORF2p-dependent *Alu* RNA-induced RPE degeneration is blocked by inhibition of reverse transcription. RPE degeneration (fundus photographs, left; ZO-1 flat mount micrographs, right) in wild-type (WT) mice after treatment with *Alu* RNA and rat L1 ORF2p-expressing in the presence or absence of high dose delavirdine (DLV; 500 pmol). Binary and morphometric quantification of RPE degeneration are shown (**P* < 0.05; ****P* < 0.001, Fisher's exact test for binary; two-tailed t-test for morphometry). PM, polymegethism (mean (SEM)). Arrowheads in fundus images denote the boundaries of RPE hypopigmentation. Scale bars, 10 μm. *n* = 6.

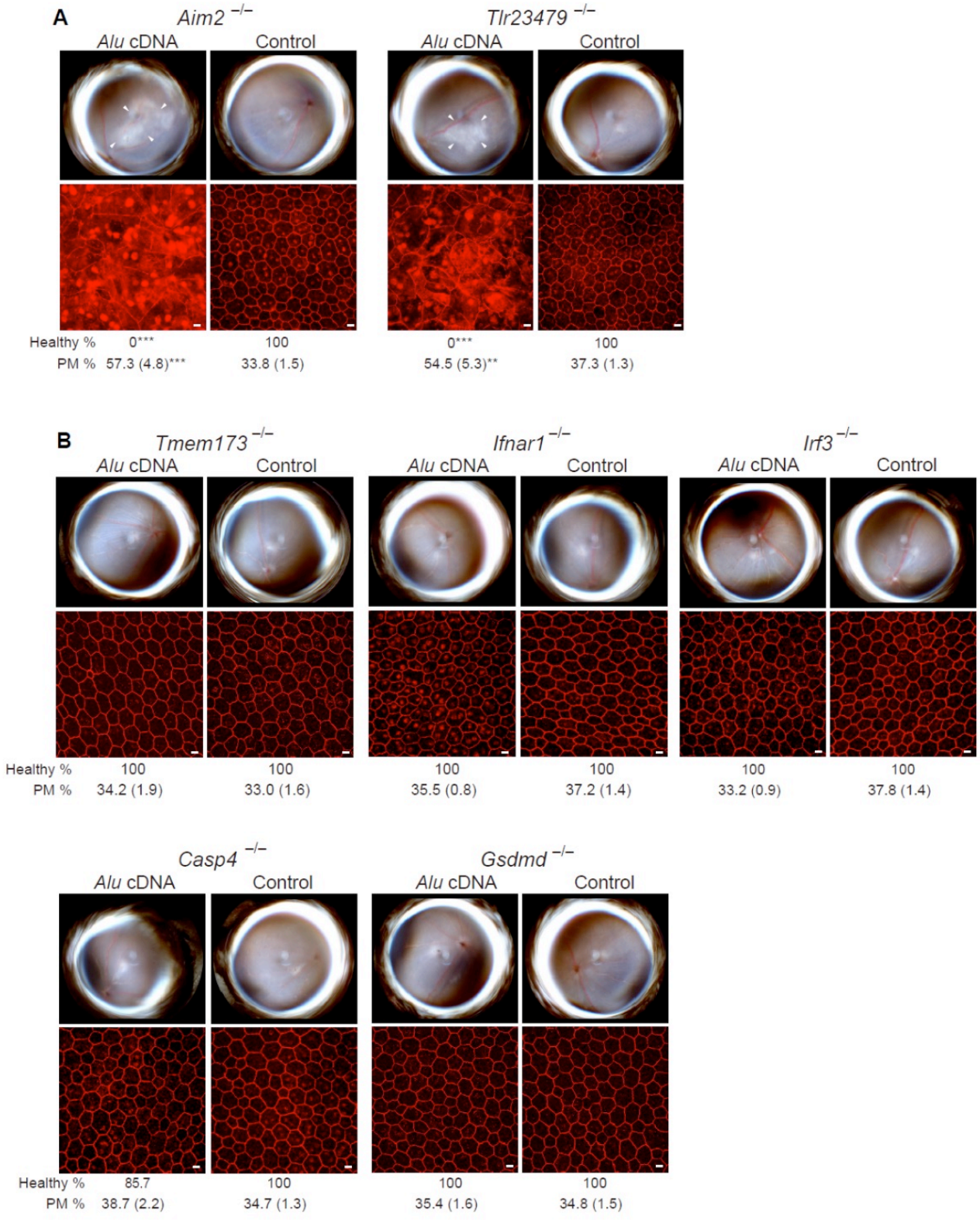
A
Aim2 −/−
Alu cDNA
Control
Tlr23479 −/−
Alu cDNA
Control
Healthy % 0*** 100 0*** 100
PM % 57.3 (4.8)*** 33.8 (1.5) 54.5 (5.3)** 37.3 (1.3)
B
Tmem173 −/−
Alu cDNA
Control
Ifnar1 −/−
Alu cDNA
Control
Irf3 −/−
Alu cDNA
Control
Healthy % 100 100 100 100 100 100
PM % 34.2 (1.9) 33.0 (1.6) 35.5 (0.8) 37.2 (1.4) 33.2 (0.9) 37.8 (1.4)
Casp4 −/−
Alu cDNA
Control
Gsdmd −/−
Alu cDNA
Control
Healthy % 85.7 100 100 100
PM % 38.7 (2.2) 34.7 (1.3) 35.4 (1.6) 34.8 (1.5)

Fig. S6. *Alu* cDNA induces RPE degeneration via the cGAS pathway. (A and **B)** RPE degeneration (fundus photos, top, and ZO-1 flat mounts, bottom) in mice after subretinal administration of *Alu* cDNA in **(A)** *Aim2*$^{-/-}$ or *Tlr23479*$^{-/-}$ mice (n = 6) and **(B)** *Alu* cDNA did not induce RPE degeneration in *Tmem173*$^{-/-}$, *Ifnar1*$^{-/-}$, *Irf3*$^{-/-}$, *Casp4*$^{-/-}$, or *Gsdmd*$^{-/-}$ mice (n = 6). Arrowheads in fundus images denote the boundaries of RPE hypopigmentation. Scale bars, 10 μm. Binary and morphometric quantification of RPE degeneration are shown (*P < 0.05; **P < 0.01; ***P < 0.001, Fisher's exact test for binary; two-tailed t-test for morphometry). PM, polymegethism (mean (SEM)).

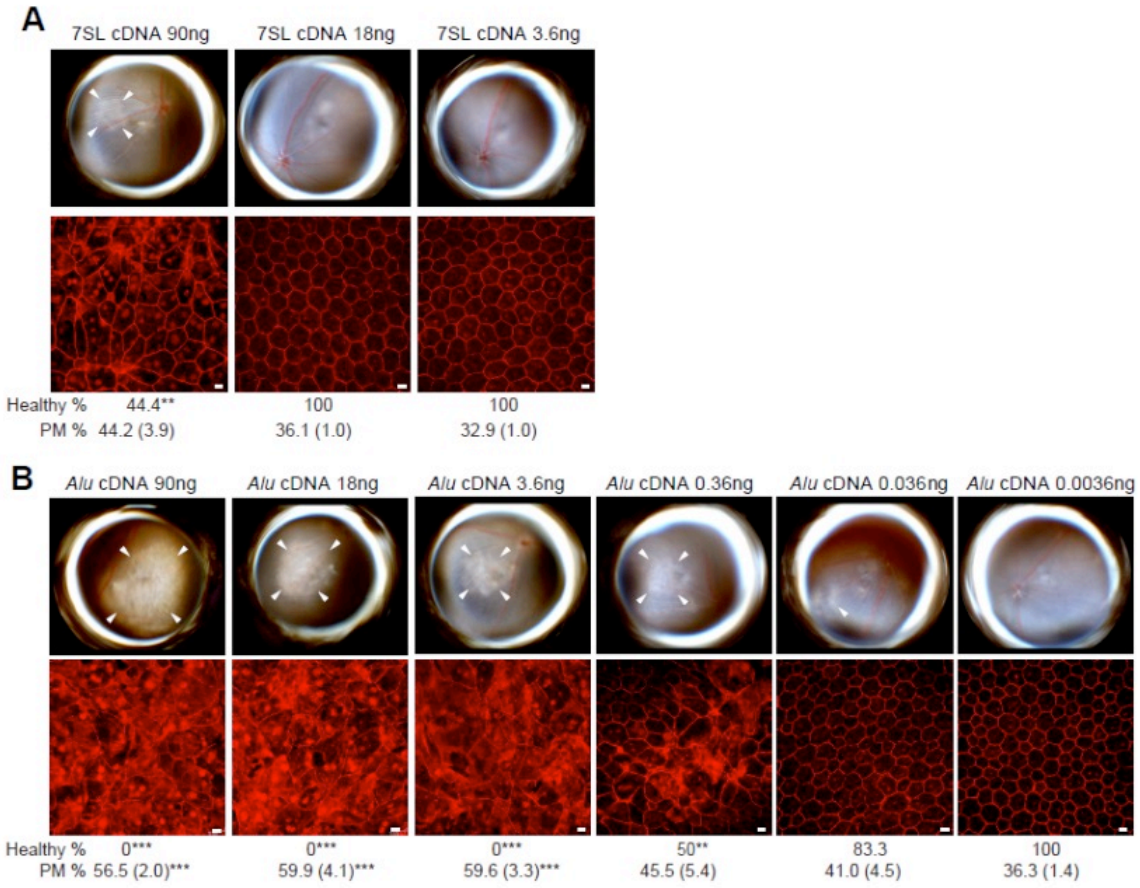

Fig. S7. Effects of 7SL cDNA and *Alu* cDNA on RPE. (**A**) RPE degeneration (fundus photos, top, and ZO-1 flat mounts, bottom) in wild-type mice after subretinal administration of a synthetic single-stranded DNA sequence complementary to 7SL RNA (7SL cDNA) at indicated doses. Note the dose required to induce RPE degeneration was 250-times greater than *Alu* cDNA (Supplementary Fig. 7B). $n = 6$. Arrowheads in fundus images denote the boundaries of RPE hypopigmentation. Scale bars, 10 μm. Binary and morphometric quantification of RPE degeneration are shown (**$P < 0.01$, Fisher's exact test for binary; two-tailed t-test for morphometry). PM, polymegethism (mean (SEM)). (**B**) Dose-ranging studies of *Alu* cDNA demonstrate its higher potency in inducing RPE degeneration compared to the potency of *Alu* RNA (Fig. S3B of (11)). $n = 6$–18.

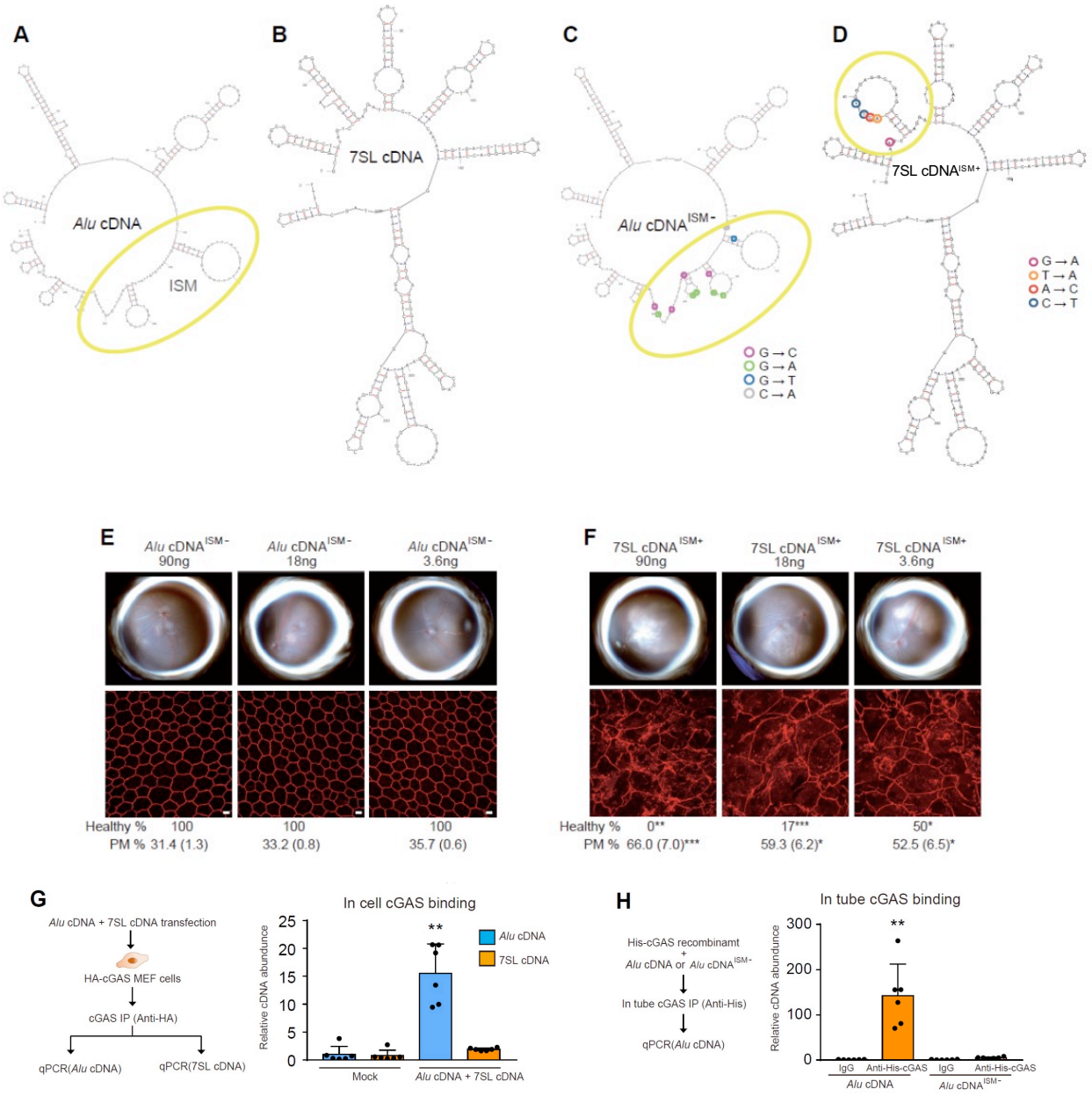

Fig. S8. Guanosine-rich immunostimulatory motif (ISM) mediates *Alu* cDNA binding cGAS and promotes RPE degeneration. (**A**) Secondary structure of *Alu* cDNA based on the mfold prediction algorithm. *Alu* cDNA contains a guanosine-rich immunostimulatory motif (ISM). Red circles denote unpaired guanosines. (**B**) Secondary structure of 7SL cDNA based on the mfold prediction algorithm. The number of unpaired guanosines was less in the 7SL cDNA than in *Alu* cDNA. (**C**) Secondary structure of the mutant form of *Alu* cDNA lacking the ISM (*Alu* cDNA$^{ISM–}$). Selected unpaired guanosines were substituted to minimize changes in the secondary structure (pink circle, guanosine → cytidine; green circle, guanosine → adenosine; blue circle, guanosine → Thymidine; gray circle, cytidine → adenosine). *Alu* cDNA$^{ISM–}$ does not harbor any unpaired guanosine. (**D**) Secondary structure of the mutant form of 7SL cDNA containing ISM (7SL cDNA^{ISM+}). Selected unpaired guanosines were substituted to minimize changes in the secondary structure (purple circle, guanosine → adenosine; orange circle,

thymidine → adenosine; red circle, adenosine → cytidine; dark blue circle, cytidine → thymidine). **(E, F)** RPE appearance (fundus photographs, top, and ZO-1 flat mount micrographs, bottom) in wild-type mice after subretinal administration of *Alu* cDNA^{ISM-} or 7SL cDNA^{ISM+}. No RPE degeneration was observed after *Alu* cDNA^{ISM-} injection at a doses 250-times greater than the dose of *Alu* cDNA required to induce RPE degeneration (Supplementary Fig. 7B). RPE degeneration was observed after 7SL cDNA^{ISM+} injection. $n = 6$. **(G)** Schematic (left) and quantification (right) of the relative binding of *Alu* and 7SL cDNAs with cGAS. *cGAS*$^{-/-}$ immortalized mouse embryonic fibroblasts (MEFs) were reconstituted with hemagglutinin (HA)-tagged cGAS and transfected with *Alu* and 7SL cDNAs. Immunoprecipitation of HA was followed by real-time PCR to quantify *Alu* and 7SL cDNAs. ** $P < 0.01$ by Mann-Whitney U test. **(H)** Schematic (left) and quantification (right) of the relative binding of *Alu* and *Alu*$^{ISM-}$ cDNAs with cGAS. Recombinant His-tagged cGAS incubated with *Alu* and 7SL cDNAs was immunoprecipitated using an anti-His tag antibody followed by real-time PCR to quantify *Alu* and *Alu*$^{ISM-}$ cDNAs. ** $P < 0.01$ by Mann-Whitney U test.

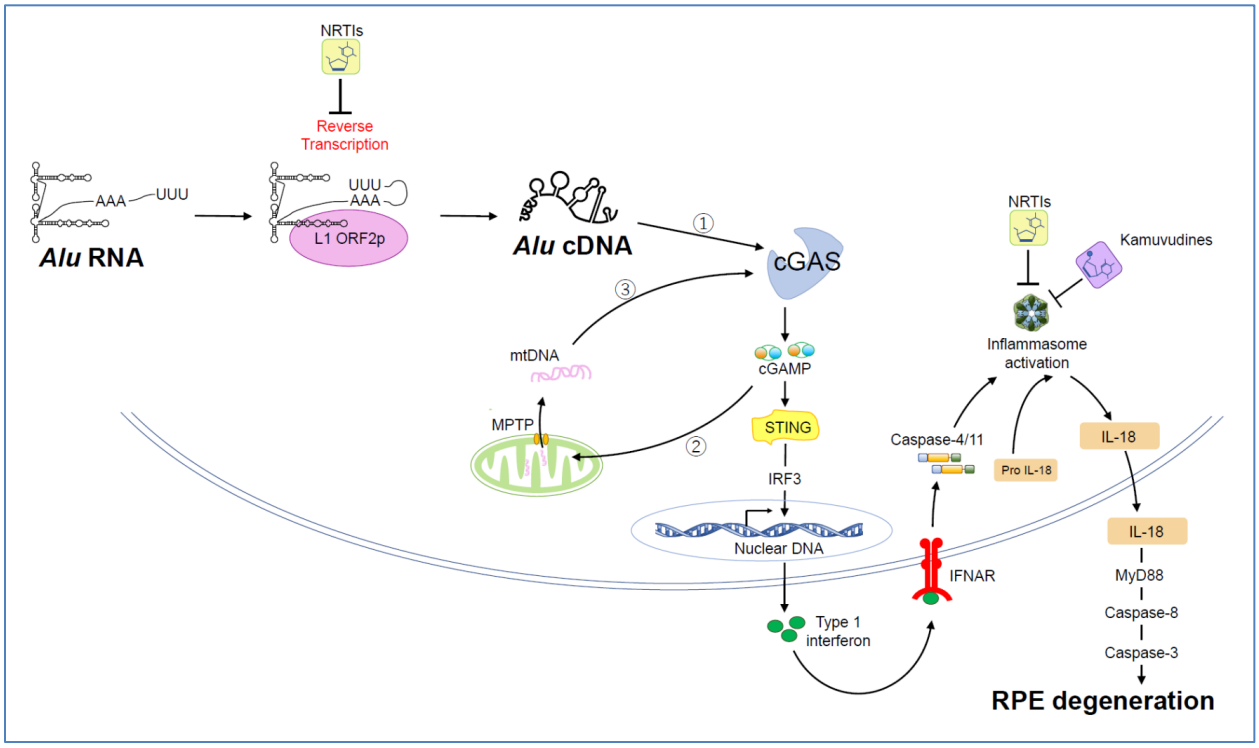

Fig. S9. Model of endogenous cytoplasmic *Alu* cDNA-induced RPE degeneration via reverse transcription and cGAS activation. *Alu* cDNA is synthesized via cytoplasmic LINE-1 ORF2p-mediated reverse transcription from *Alu* RNA. Reverse transcription occurs by self-priming. *Alu* cDNA employs cGAS to induce mitochondrial DNA (mtDNA) release, which subsequently amplifies cGAS activation. cGAS-driven type I interferons (IFNs) triggers caspase-4/11 activation and NLRP3 inflammasome-mediated secretion of IL-18. The autocrine and paracrine IL-18 signaling leads to RPE cell death via Myd88, Caspase-8 and Caspase-3.

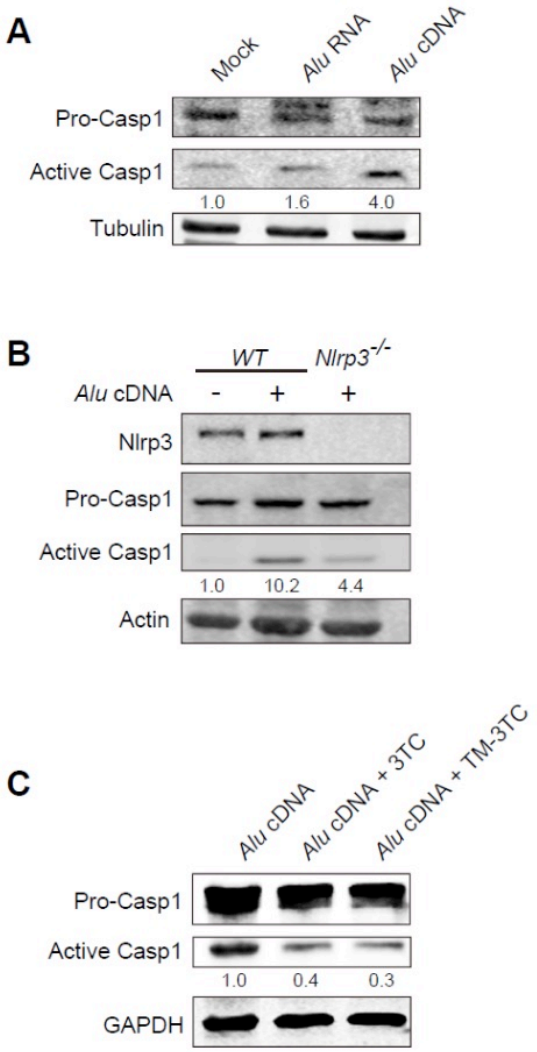

Fig. S10. Caspase-1 activation by *Alu* RNA and *Alu* cDNA. (**A**) Immunoblotting analysis of caspase-1 activation in primary human RPE cells transfected with in vitro transcribed *Alu* RNA or *Alu* cDNA. (**B**) Immunoblotting analysis of caspase-1 activation in *Alu* cDNA-transfected WT and *Nlrp3*$^{-/-}$ BMDMs. (**C**) Immunoblotting analysis of caspase-1 activation in *Alu* cDNA-transfected ARPE-19 cells treated with 3TC or trimethyl-3TC (TM-3TC). Densitometry of normalized active caspase-1 values shown below lanes.

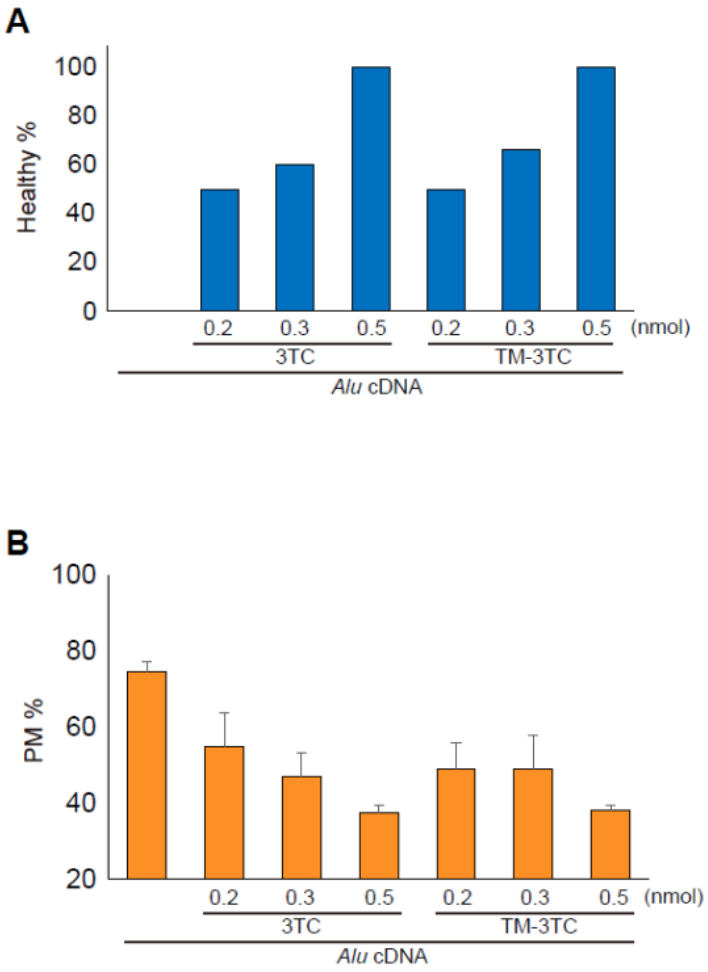

Fig. S11. Dose-dependent effect of 3TC and trimethyl-3TC (TM-3TC) on *Alu* cDNA-induced RPE degeneration in WT mice. (**A**) Binary and (**B**) morphometric quantification of RPE degeneration. PM, polymegethism (mean ± SEM). n = 5–6.